E-ISSN 2586-9027
Homepage : https://tci-thaijo.org/index.php/SciTechAsia Science & Technology Asia
Vol.30 No.3 July - September 2025 Page: [120-127]
Original research article

Is Change of Spin State Critical for 3d Transition Metal Carbon Monoxide Bonding?

Natthakrij Nipanutiyan, Kaito Takahashi*

Sirindhorn International Institute of Technology, Thammasat University, Pathum Thani 12120, Thailand

Received 7 June 2025; Received in revised form 23 July 2025
Accepted 18 August 2025; Available online 30 September 2025

ABSTRACT

Transition metal carbonyl (TM-CO) interaction is seen in different areas, including catalysts for CO_2 reduction and biological processes involving CO gas. Due to the complex occupation of 3d orbitals, the spin state can change when a TM binds with various gas molecules. In this study, we evaluated the simplest of such spin crossover reactions: 3d TM atom + CO in detail using B3LYP/6-31+G(d,p). Previous studies on TM-CO by Fournier evaluated the dissociation limit and adduct energies and compared spin states. In the present study, we extended the study to include the calculation of the association potential energy curve. We focused on finding the crossing point of two spin states as a function of the TM-C bond length. We also evaluated the relationship between the change of spin state and stable binding between the TM atom and the CO molecule. We found that Sc, Ti, Fe, Co, and Ni + CO are candidates to be spin crossover reactions that change spin upon TM-CO bond formation. Furthermore, among the 3d TM atoms, the most strongly binding TM atoms were Ni, Ti, Fe, and Co, which showed spin state change upon bonding.

Keywords: Density functional theory; Potential energy curve; Spin crossover; Transition metal

1. Introduction

The bonding between a transition metal (TM) atom and carbon monoxide (CO) is important in various areas, such as catalysis for CO_2 reduction, CO detection, and clinical applications for CO. Pauling and Coryell discovered a spin state change, or spin crossover, when CO binds to a heme-related iron-porphyrin complex [1]. Before CO binding, the heme complex ex-

***Corresponding author:** kaitot@siit.tu.ac.th **doi:** 10.14456/scitechasia.2025.54

hibited magnetic properties; however, after CO binding, it did not interact with magnets. To gain an understanding of this interesting spin crossover interaction, various studies have evaluated the simplest system: the association of a TM atom and CO.

Many 3d TM-CO [2-12] adducts have been synthesized, and infrared CO stretching peak shifts have suggested a change in bonding interaction upon metal-ligand bond formation. Furthermore, various theoretical studies have also evaluated the binding interaction [13-16]. Fournier used density functional theory (DFT) to calculate the TM and CO energies at the dissociation limit and the adduct TM-CO bonded geometry [14]. Interestingly, he found that late TM atoms, such as Mn, Fe, Co, and Ni, have stable high-spin states at atomic electron configurations, but when forming a TM-CO bond, the low-spin state becomes stable. On the other hand, for early TMs, such as Sc, Ti, and V, the low-spin state is most stable at the atomic configuration, but a high-spin state is more stable upon TM-CO bond formation. Fournier discussed such differences in spin state, but did not calculate the potential energy curve (PEC) to evaluate the spin crossover point. On the other hand, Rosesomme et al. evaluated the PEC of TM-CO associations using DFT, but focused on systems that have a stable singlet spin state [13].

DFT calculations can show which spin state is lower at a given nuclear geometry, but to properly confirm if spin crossover is possible, one needs to evaluate multiple spin state PECs involving a multiconfigurational spin-orbit interaction calculation. However, such calculations are very expensive and usually not performed. In most cases, 3d TM atoms are assumed to have strong spin-orbit coupling, which will result in a spin state change or spin crossover. Recently, one of the authors evaluated the Ni-CO association using multireference spin-orbit calculation [17], and showed that spin crossover occurs at a Ni-C bond distance of 2.2-2.4 $\mathring{A}$, slightly longer than the equilibrium singlet Ni-CO bond length of 1.65 $\mathring{A}$. A key finding from this paper is that the spin-orbit coupling value begins to decrease as the Ni-C bond length is shortened below 2.1 $\mathring{A}$, where the Ni-CO bonding becomes stronger. Therefore, spin-orbit interaction is also sensitive to the TM-C bond length. Therefore, it is important to determine the TM-C bond length at which the two spin state energies cross. An interesting finding from this study on the Ni-CO association PEC is that the spin-crossover Ni-C bond length, as determined using multireference methods and hybrid DFT functionals, was the same. Furthermore, this multireference calculation showed that at the dissociation limit and the NiCO adduct bound geometries, the electronic state can be given by a single electronic configuration. Indeed, hybrid DFT functionals were able to give Ni-CO binding energies that reproduced experimental values. Therefore, as a starting point to evaluate spin crossover reactions, PEC calculations using hybrid DFT methods would help us determine which TM-C bond length to focus our multireference calculation on for each TM. Takahashi recently compared the PECs of Sc-CO and Ni-CO bond formation using DFT methods and showed that the spin crossover point differs between the two TM atoms [18]. However, we do not find any study on the other 3d TM atoms.

In conclusion, the spin crossover reaction is effective in the association of 3d TM atoms and CO. Thereby, clarifying the crossing point along the TM-C bond length would be beneficial for future mutireference studies for 3d TM atoms. Further-

more, considering the importance of spin for 3d TMs, we would like to ask if spin state change would lead to a stronger bond between 3d TM atom and CO. We utilized hybrid DFT methods to evaluate the association PEC for 3d TM and CO and compared the binding energy of 3d TM carbonyl complexes.

2. Methods

We calculated the PECs of various possible spin states for 3d TM-CO association using unrestricted Kohn-Sham DFT. Therefore, open-shell singlet states were also included in our study. We used Becke's three parameter hybrid functional (B3LYP) [19, 20] with Pople's 6-31+G(d,p) basis set [21] implemented in the Gaussian16 program [22]. We first calculated an isolated 3d TM atom and a CO molecule, then optimized the linear TM-CO complex. Calculations were performed for all possible spin states, and the equilibrium TM-C bond distances are given in Table 1. Zn has a $4s^2\ 3d^{10}$ closed-shell configuration, and we could not find a stable bound Zn-CO geometry; therefore, it is ignored here. After obtaining the stable adduct, we calculated the collinear association potential energy curve of the TM-C bond length for the 2 low-lying spin states, while fixing the C-O bond length. For each TM, the C-O bond length was fixed to the average of the adduct C-O bond length of the 2 spin states. We note that a proper evaluation would require a 3-dimensional potential energy surface involving changes in TM-C and C-O bond lengths as well as the TM-C-O angle. However, as discussed later, this effect is likely to be less than 0.05 eV. In the present study, we focus on the collinear association. For the various 3d TM atoms, we calculated the potential energy from TM-C equilibrium distance Req -0.1 to Req+2.0 Å in grid intervals of 0.1 Å and from Req+2.0 Å to 8.0 Å in grid intervals of 0.25 Å. Considering the complex electronic state of the PEC, we performed the bond length scan calculation in both directions, elongating and shortening the TM-C bond. The PECs presented in the current manuscript are the lowest energy curves obtained from this dual direction potential energy scan. For some TM atoms, we altered the orbital occupation to obtain the desired electron configuration. In the present study, we neglected the zero-point vibration and reported only the electronic energy along the PEC.

Table 1. Energy of B3LYP before and after bonding for each spin multiplicity in eV, and geometries of the adduct given in Å.

System		TM-C bond length (Å)	C-O bond length (Å)	Adduct Energy (eV)	Dissociation limit Energy (eV)
Element	Multiplicity				
Sc	Doublet	2.21	1.15	-0.29	0.00
	Quartet	2.09	1.17	-0.72	0.96
Ti	Triplet	2.02	1.17	-0.86	0.00
	Quintet	2.04	1.17	-1.28	0.05
V	Quartet	1.91	1.18	-0.36	0.18
	Sextet	1.99	1.16	-1.08	0.00
Cr	Quintet	2.03	1.15	0.18	0.79
	Septet	2.19	1.16	-0.23	0.00
Mn	Quartet	1.91	1.16	0.60	2.06
	Sextet	2.03	1.16	0.33	0.00
Fe	Triplet	1.76	1.16	-1.20	0.43
	Quintet	1.91	1.16	-1.07	0.00
Co	Doublet	1.70	1.16	-1.13	0.28
	Quartet	1.90	1.15	-0.71	0.00
Ni	Singlet	1.68	1.16	-1.52	0.13
	Triplet	1.90	1.14	-0.49	0.00
Cu	Doublet	1.95	1.14	-0.23	0.00
	Quartet	1.92	1.18	3.41	5.49

3. Results and Discussion

3.1 Comparison of 3d TM-CO energies

In Table 1, we present the dissociation limit and the electronic energy of the adduct for various 3d TM-CO complexes. For each TM, the zero of energy is set at the most stable dissociation limit spin state (TM + CO), and the more negative the adduct energy is, the stronger the TM bonding. Con-

sistent with Fournier's results, we found that for early transition metals, such as Sc, Ti, V, Cr, and Mn, the high-spin state is more stable at adduct geometries. On the other hand, for late TM atoms, such as Fe, Co, Ni, and Cu, the low-spin state is more stable at the adduct geometry.

In addition to the trend of stable spin states for early and late TMs, we also observe spin state changes for some of them. As shown in Table 1, early TM, such as Sc and Ti, increase in spin multiplicity when forming a TM-CO bond, whereas late TM, Fe, Co, and Ni, decrease in spin multiplicity when the TM-CO bond is formed.

We also present the TM-C and C-O bond lengths of the adduct complex. Considering that the isolated CO has a bond length of 1.13 $\mathring{A}$, TM-CO bonding has increased the CO bond length. This is consistent with the experimentally observed change in the CO stretching frequency and is attributed to the π-back donation from the TM 3d orbital to the CO $\pi^{\star}$ orbital. Such orbital interaction results in a weakened and elongated CO bond. We also present the TM-C bond lengths, and it can be seen that Fe, Co, and Ni are shorter than the other TMs.

3.2 Potential energy curve

In this section, we evaluate the association PEC for 3d TM atoms that have spin state change upon CO binding. In Figs. 1-2, we present the results for Sc and Ti, respectively. The results for the late TM atoms: Fe, Co, and Ni, are given in Figs. 3 to 5. Before discussing each PEC, we can confirm that for all TM-CO binding, the PECs plateau beyond the TM-C bond length of 6 $\mathring{A}$. This signifies that the interaction between the TM and CO is negligible beyond this bond length. Furthermore, we can confirm that the relative energies at adduct geometry and at TM-C 6 $\mathring{A}$ match the energies given in Table 1. This helps us confirm that we have calculated the correct electronic configuration.

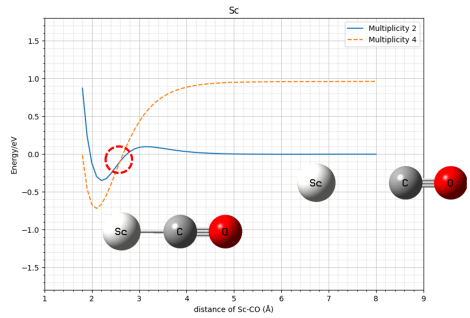

Fig. 1. Association potential energy curve of Sc-CO, as a function of Sc-CO bond distance. The results for multiplicities 2 and 4 are presented in blue solid and orange dashed lines, respectively. Schematic geometries are also presented.

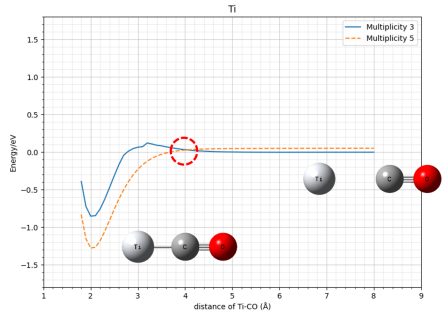

Fig. 2. Association potential energy curve of Ti-CO, as a function of Ti-CO bond distance. The results for multiplicities 3 and 5 are presented in blue solid and orange dashed lines, respectively.

One can clearly see that before the association at long Sc-C bond lengths, the doublet spin state is much more stable, but as the Sc-CO bond is formed, the quartet state decreases significantly in energy. We observe a spin crossover at the TM-C bond length of 2.6 $\mathring{A}$. On the other hand,

for Ti, the energy difference between the triplet and quintet states at the dissociation limit is very small. Interestingly, for Ti, the crossover occurs at a very long Ti-C bond length of 4.0 $\mathring{A}$. Moving on to the late

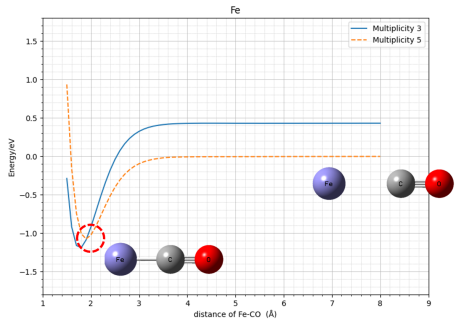

Fig. 3. Association potential energy curve of Fe-CO, as a function of Fe-C bond length. The results for multiplicities 3 and 5 are presented in blue solid and orange dashed lines, respectively.

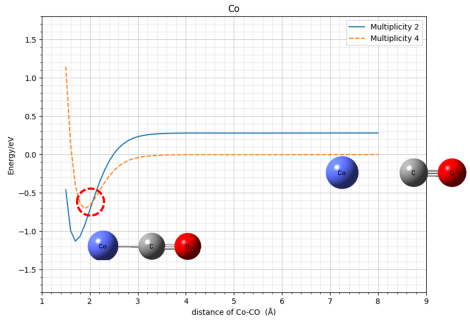

Fig. 4. Association potential energy curve of Co-CO, as a function of Co-C bond length. The results for multiplicities 2 and 4 are presented in blue solid and orange dashed lines, respectively.

TMs, we focus on the results in Figs. 3-5. Here we see that for Fe and Co, the crossover TM-C bond length is very close to the higher spin state minima. This differs from Sc and Ti, as shown in Figs. 1-2. Correspondingly, the spin crossover point is at a shorter TM-C bond length of 2.0 $\mathring{A}$ for Fe and Co. As discussed in our pre-

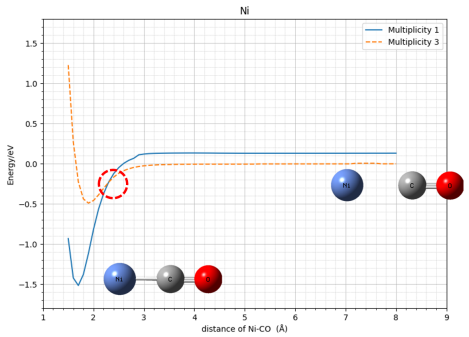

Fig. 5. Association potential energy curve of Ni-CO, as a function of Ni-C bond length. The results for multiplicities 1 and 3 are presented in blue solid and orange dashed lines, respectively.

vious multireference calculation for NiCO [17], the spin-orbit interaction is critical for the change in spin states. Even if the PECs of 2 different spin states cross, if the spin-orbit coupling is small at that geometry, we will not have spin crossover. Our previous studies showed that for NiCO, the spin-orbit interaction is strong in the vicinity of the singlet-triplet PEC crossing, so spin crossover is active. It was also found that spin-orbit interaction is larger when the system has atomic characteristics. Therefore, spin crossover is more favorable for TM-CO systems that have two spin states crossing at long TM-CO distances. With this in mind, we can predict that the spin crossover may not be very effective for Fe and Co, which have spin state crossing at the minima geometry of the high-spin state. However, further calculations using multireference spin-orbit interaction are needed to confirm this issue.

Before ending this section, we comment on the possible errors of using a fixed C-O bond length and a linear association pathway. To balance the effect of 2 spin states, we fixed the C-O bond length as the average of the TMCO adduct geometry for these states. We placed the zero of energy

for the PEC to be the lowest energy spin state at the TM-C distance of 8 $\mathring{A}$. If we evaluate the minimum energy of the PECs given in Figs. 1-5, we obtain -0.72, -1.28, -1.19, -1.13, and -1.51 for Sc, Ti, Fe, Co, and Ni, respectively. We can see that these values are within 0.01 eV of the optimized binding energies given in Table 1. Therefore, we can confirm that the error of using a fixed C-O bond length will be minor.

Next, the TM-C-O angle was assumed to be linear in the PEC calculation. Previous computational studies by Pilme et al. [23], have found that most 3d TMCO adduct complexes are, in fact, linear. According to their study, the weak binding spin states of CrCO, CoCO, NiCO, and CuCO complexes are bent. We performed further B3LYP calculations and confirmed this. However, we found that the difference between linear and bent geometries is -0.12, -0.03, -0.03, and -0.20 eV for CrCO, CoCO, NiCO, and CuCO, respectively. Therefore, we believe that the crossing point given in Figs. 4-5 for Co and Ni may be affected by other degrees of freedom, but this effect is likely to be within 0.05 eV by adding the 0.01 eV for fixed C-O bond length and 0.03 eV for bending.

3.3 Comparison of spin state change and binding energy

In the previous section, we evaluated the PEC of systems with spin crossover. In this section, we evaluate if the existence of spin crossover is important for the CO binding or not. In Table 2, we align the various 3d TM in order of stronger TM-CO binding energy. Interestingly, we can see that the 4 strongest CO binding TM atoms, Ni, Ti, Fe, and Co, all show spin crossover reactions. On the other hand, the 3 weakest binding TM, Cr, Cu, and Mn, all keep their spin state as the TM-CO bond is formed. Therefore, we see that a change in electron orbital occupation involving a spin state change is critical for the binding of CO to 3d TM atoms. As Fournier mentioned, this is related to the key electron configuration for the TM-CO bond state, which differs from that of the isolated TM atoms. Most isolated 3d TM atoms take a $4s^2\ 3d^n$ electron configuration. On the other hand, the highest occupied molecular orbital (HOMO) of CO is a σ-orbital with a large electron distribution on the carbon side. Therefore, TM-CO association results in a strong repulsion between the CO HOMO and the TM 4s orbital. Thus, at the TM-CO adduct geometry, the TM favors $4s^1\ 3d^{n+1}$ or $4s^0\ 3d^{n+2}$ electron configurations. In essence, to achieve stable TM-CO adduct formation, the electron configuration of the 3d TM must reduce σ-repulsion by reducing the occupation in the 4s orbital, resulting in a spin state change for the four strong-binding TM atoms: Ni, Ti, Fe, and Co.

Table 2. 3d TM in the order of strong to weak binding, and whether spin state changes or not.

System	Spin state change	Binding energy (eV)
Ni	Yes	-1.52
Ti	Yes	-1.28
Fe	Yes	-1.20
Co	Yes	-1.13
V	No	-1.08
Sc	Yes	-0.72
Cr	No	-0.23
Cu	No	-0.23
Mn	No	0.33

4. Conclusion

We evaluated the possibility of spin crossover for the association of 3d TM atoms and CO using B3LYP/6-31+G(d,p). Similar to previous studies by Fournier, we find that early TM atoms tend to favor high spin states upon TM-CO bond formation, while later TM atoms favor low spin states. We found that Sc, Ti, Fe, Co, and Ni +

CO can undergo spin crossover reactions, changing spin upon formation of the TM-CO bond. Interestingly, for Fe and Co, the spin crossover TM-C bond length occurs near the minimum of the higher energy high-spin state. Further studies using multi-configurational spin-orbit calculations are needed to confirm if spin crossover can occur in these late TMs. Furthermore, among the 3d TM atoms, the strongest binding TM were Ni, Ti, Fe, and Co, which showed spin state change. This suggests that spin crossover is crucial for strong TM-CO binding, and we believe this is linked to the electron configuration change from atomic $4s^2$ $3d^n$ orbital occupation to $4s^1$ $3d^{n+1}$ or $4s^0$ $3d^{n+2}$ occupation upon TM-CO bond formation.

Acknowledgements

We acknowledge support from the Institute of Atomic and Molecular Sciences, Academia Sinica, Taiwan, and Sirindhorn International Institute of Technology, Thammasat University, Thailand. KT thanks the Young Researcher Grant from Sirindhorn International Institute of Technology, Thammasat University (SIIT-2024-YRG-KT02).

References

[1] Pauling L, Coryell CD. The magnetic properties and structure of hemoglobin, oxyhemoglobin and carbonmonoxyhemoglobin. Proc Natl Acad Sci U S A. 1936;22(4):210-6.

[2] DeKock RL. Preparation and identification of intermediate carbonyls of nickel and tantalum by matrix isolation. Inorg Chem. 1971;10(6):1205-11.

[3] Kündig EP, McIntosh D, Moskovits M, Ozin GA. Binary carbonyls of platinum, Pt(CO)n (where n = 1-4). Comparative study of the chemical and physical properties of M(CO)n (where M = nickel, palladium, or platinum; n = 1-4). J Am Chem Soc. 1973;95(22):7234-41.

[4] Huber H, Kündig EP, Ozin GA, Poe AJ. Reactions of monatomic and diatomic manganese with carbon monoxide. Matrix infrared spectroscopic evidence for pentacarbonylmanganese Mn(CO)5 and the binuclear carbonyls Mn2(CO)n (where n = 1 or 2). J Am Chem Soc. 1975;97(2):308-14.

[5] Hanlan LA, Huber H, Kündig EP, McGarvey BR, Ozin GA. Chemical synthesis using metal atoms. Matrix infrared, Raman, ultraviolet-visible, and electron spin resonance studies of the binary carbonyls of cobalt, Co(CO)n (where n = 1-4), and the distortion problem in tetracarbonylcobalt. J Am Chem Soc. 1975;97(24):7054-68.

[6] Tremblay B, Alikhani ME, Manceron L. The Co + CO reaction: Infrared matrix isolation study and density functional calculations. J Phys Chem A. 2001;105(50):11388-94.

[7] Huber H, Kündig EP, Moskovits M, Ozin GA. Binary copper carbonyls. Synthesis and characterization of tricarbonylcopper, dicarbonylcopper, monocarbonylcopper, and hexacarbonyldicopper. J Am Chem Soc. 1975;97(8):2097-106.

[8] Hanlan L, Huber H, Ozin GA. Direct synthesis using vanadium atoms. 3. Binary carbonyls of vanadium, V(CO)n (where n = 1-5). Inorg Chem. 1976;15(11):2592-7.

[9] Engelking PC, Lineberger WC. Laser photoelectron spectrometry of the negative ions of iron and iron carbonyls. Electron affinity determination for the series Fe(CO)n, n = 0-4. J Am Chem Soc. 1979;101(19):5569-73.

[10] Peden CHF, Parker SF, Barrett PH, Pearson RG. Moessbauer and infrared studies of matrix-isolated iron-carbonyl complexes. J Phys Chem. 1983;87(13):2329-36.

[11] Stevens AE, Feigerle CS, Lineberger WC. Laser photoelectron spectrometry of Ni(CO)n-, n = 1-3. J Am Chem Soc. 1982;104(19):5026-31.

[12] Tanaka K, Sakaguchi K, Tanaka T. Time-resolved infrared diode laser spectroscopy of the v1 band of the iron carbonyl radical (FeCO) produced by the ultraviolet photolysis of Fe(CO)5. J Chem Phys. 1997;106(6):2118-28.

[13] Rossomme E, Lininger CN, Bell AT, Head-Gordon T, Head-Gordon M. Electronic structure calculations permit identification of the driving forces behind frequency shifts in transition metal monocarbonyls. Phys Chem Chem Phys. 2020;22(2):781-98.

[14] Fournier R. Theoretical study of the monocarbonyls of first-row transition metal atoms. J Chem Phys. 1993;99(3):1801-15.

[15] Blomberg MRA, Brandemark UB, Siegbahn PEM, Wennerberg J, Bauschlicher CW. The nickel-carbonyl binding energy in Ni(CO)x (x = 1-4). A theoretical investigation. J Am Chem Soc. 1988;110(20):6650-5.

[16] Frenking G, Pidun U. Ab initio studies of transition-metal compounds: The nature of the chemical bond to a transition metal. J Chem Soc Dalton Trans. 1997;(10):1653-62.

[17] Yoshida D, Takahashi K. Multistate transition metal carbonyl bonding beyond minimum energy pathway: Nonlocality of spin–orbit interaction. Inorg Chem. 2025;64(1):286-94.

[18] Takahashi K. Origin of spin crossover in the association of carbon monoxide and transition metal atoms. PACCON2025 e-Proceedings. 2025;1.

[19] Becke AD. Density-functional thermochemistry. III. The role of exact exchange. J Chem Phys. 1993;98(7):5648-52.

[20] Lee C, Yang W, Parr RG. Development of the Colle-Salvetti correlation-energy formula into a functional of the electron density. Phys Rev B. 1988;37(2):785-9.

[21] Krishnan R, Binkley JS, Seeger R, Pople JA. Self-consistent molecular orbital methods. XX. A basis set for correlated wave functions. J Chem Phys. 1980;72(1):650-4.

[22] Frisch MJ, Trucks GW, Schlegel HB, Scuseria GE, Robb MA, Cheeseman JR, et al. Gaussian 16, Revision A.03. Wallingford CT: Gaussian Inc.; 2016.

[23] Pilme J, Silvi B, Alikhani ME. Structure and stability of M−CO, M = first-transition-row metal: An application of density functional theory and topological approaches. J Phys Chem A. 2003;107(22):4506-14.